KTH Industrial Engineering and Management

Potential of harvesting solar neutrinos to power electric cars

Michael Hoenes

Master of Science Thesis
KTH School of Industrial Engineering and Management
Energy Technology TRITA-ITM-EX 2019:639
SE-100 44 STOCKHOLM

KTH Industrial Engineering and Management

Master of Science Thesis TRITA-ITM-EX 2019:639

Potential of harvesting solar neutrinos to power electric cars

Michael Hoenes

Approved	Examiner	Supervisor
	Viktoria Martin	Thomas Nesch
	Commissioner	Contact person

Sammanfattning

Pa grund av överhängadne bestraffningar för överskottsutsläpp behöver bilindustrin hitta ny sätt att driva sina bilar. För att göra detta behöver man hitta nya koncept vilka exempelvis kan hittas genom att leta efter patent fran nystartade och etablerade företag.

Daimler AG har under sitt sökande efter patent kommit över ett patent fran start-up-företaget Neutrino Energy GmbH. De har tagit fram en maskin designad för att skörda solneutrioner och med hjälp av dessa generera el. Detta väcker fragan: Är det möjligt att skörda solneutrinos för att försörja elkonsumenter, sa som bilar, med el?

Den här studien besvarar den här fragan genom att analysera flödet av solneutriner pa jordytan samt den mordernaste solneutrinotekniken (inklusive solneutrino-detektorer som används i forskning och den solneutrinomvandlare som föreslagits av Neutrino Energy GmbH).

Beräkningarna för den inneboende energin i solneutinoflödet är baserade pa solneutiospektrum som aterfinns i litteraturen. Solneutrinodetektorers förmaga att skörda solneutriner analyseras genom litteratur och uppskattning av deras effekt. När det kommer till den grafenbaserade omvandlaren från Neutrino Energy GmbH, jämförs tröskelenergierna för neutrino-grafeninteraktioner med energin från inkommande neutrino för att uppskatta en övre gräns för den utgaende effekten.

Resultaten från analysen av solneutrino-flödet visar att den inneboeande energin i solneutriner är för låg för att driva ett elektriskt fordon, även om den skulle kunna utnyttjas fullt ut. I själva verket kan bara en liten del av energin fran solneutrinoflödet omvandlas till elektricitet eftersom neutrinos knappt interagerar med materia.

Analysen av toppmodern solneutrino-forskning visar att detektorer med en vikt på flera ton är konstruerade för att fånga signaler från solneutrino. Trots det är effektutgången från sådana detektorer flera ganger lägre än vad som krävs för en elbil. Analysen av det konceptet som Neutrino Energy GmbH utvecklat visar att endast en liten del av solneutrino-flödet kan skördas, otillräcklig för att generera en signifikant mängd el.

Därför dras slutsatsen att tekniken för att omvandla enerigin i solneutriner till el inte är någon lämplig kandidat för att möjliggöra hållbar bilindustri.

Abstract

Imminent penalties for excess emissions force the automotive industry to radically rethink how to power vehicles. Novel concepts are needed to facilitate these changes, which might be found by scouting patents of emerging and established companies.

During their patent search, Daimler AG has come across a patent of the startup Neutrino Energy GmbH, which reveals a device designed to harvest solar neutrinos for electricity generation purposes. From here the question arises: Is it possible to harvest solar neutrinos to power electric consumers, such as cars?

To answer this question, this study analyzes the solar neutrino flux on Earth's surface and the state-of-the-art solar neutrino technology (including solar neutrino detectors used in research and the solar neutrino converter proposed by Neutrino Energy GmbH). The energy inherent to the solar neutrino flux is computed based on the solar neutrino spectrum found in literature. Solar neutrino detectors are analyzed on their ability to harvest solar neutrinos by consulting literature and by estimating their power output. In case of the graphene based converter by Neutrino Energy GmbH, the threshold energies of neutrino-graphene interactions are compared to the energies of incoming neutrinos to estimate an upper limit for the power output.

Results from the analysis of the solar neutrino flux show that the energy inherent to solar neutrinos is too low to power an electric vehicle, even if it could be fully exploited. In fact, only a tiny fraction of the solar neutrino energy flux can be converted into electricity as neutrinos barely interact with matter.

The analysis of the state-of-the-art solar neutrino research shows that detectors with a weight of several tonnes are constructed to capture signals from solar neutrinos. Still, the power output of such detectors is several orders of magnitude lower than the demand of an electric vehicle. Analyzing the concept developed by Neutrino Energy GmbH shows that only a small part of the solar neutrino flux can be harvested, insufficient to generate a significant amount of electricity.

Hence, the conclusion is drawn, that solar neutrino conversion technology is no suitable candidate to enable sustainable mobility.

Contents

List of Figures vii

List of Tables viii

Nomenclature ix

1 Introduction 1

1.1 The demand for sustainable mobility 1

1.2 Neutrinos: astronomical carriers of energy 2

1.3 Objectives 4

1.4 Limitations 4

2 Solar neutrinos 5

3 State-of-the-art solar neutrino technology 9

3.1 Solar neutrino detectors 9

3.1.1 Radiochemical detectors 12

3.1.2 Water Cherenkov technique 15

3.1.3 Scintillation detectors 17

3.2 Solar neutrino energy converters 19

4 Methodology 22

4.1 Energy need of electric vehicles 22

4.2 Energy flux through neutrino irradiation 23

4.3 Analysis of the state-of-the-art 25

4.3.1 Analysis of solar neutrino detectors 25

4.3.2 Analysis of the neutrino energy converter 27

5 Results **28**
5.1 Results from calculation of the energy flux through neutrino irradiation . 28
5.2 Results from analysis of the state-of-the-art 29
5.2.1 Results from analysis of solar neutrino detectors 29
5.2.2 Results from analysis of the neutrino energy converter 31

6 Discussion and conclusions **34**

7 Outlook **36**

Bibliography **I**

Acknowledgements **V**

List of Figures

2.1 Solar neutrino spectrum for the solar model BS05(OP). 7

3.1 Scheme of the GALLEX detector tank. 14
3.2 Cherenkov light emission. 15
3.3 Cross-section through the Borexino detector. 18
3.4 Scheme of the invention described in the patent. 20
3.5 Multilayer coating of the aluminum base. 21

4.1 Plot of solar neutrino flux data obtained via WebPlotDigitizer and from Bahcall. 23
4.2 Differential electron recoil spectra in liquid xenon. 27

5.1 Solar neutrino energy spectrum with lowest threshold for neutrino-carbon interaction. 32

List of Tables

2.1 Solar neutrino fluxes (Φ) with uncertainties as calculated by John N. Bahcall. 6

3.1 Neutrino absorption cross sections averaged over energy spectra, as calculated by J. N. Bahcall. 10
3.2 Neutrino-electron scattering cross sections. 11
3.3 List of selected solar neutrino experiments sorted by their operating time. 11

4.1 Integration boundaries for each neutrino branch. 24
4.2 Neutrino capture and event rates for chosen neutrino branches in GALLEX. 25

5.1 The calculated neutrino fluxes are shown and compared to reference values. 28
5.2 The energy fluxes obtained from the different solar neutrino branches are listed. 29
5.3 The detectors, which where presented earlier are listed with their target material weight (m_{t}). 30
5.4 The detectors, which where presented earlier are listed with their neutrino detection threshold energies (E_{th}). 30
5.5 The specific power P' for DARWIN is given in W/t for the pp and ^{7}Be-neutrino branches. 31

Nomenclature

Acronyms

APPEC	Physics European Consortium
BEV	battery electric vehicle
CNO	carbon-nitrogen-oxygen
eV	electronvolt
IPCC	Intergovernmental Panel on Climate Change
LNGS	Laboratori Nazionali del Gran Sasso
PMT	photomultiplier
pp	proton-proton
SNO	Sudbury Neutrino Observatory
SNU	solar neutrino unit
SURF	Sanford Underground Research Facility

Symbols

A	-	mass number
e^+	-	positron
e^-	-	electron
n	-	neutron
p	-	proton
P_ν	$\mathrm{W\,m^{-2}}$	neutrino energy flux
P'	$\mathrm{W\,t^{-1}}$	specific power
q	eV	neutrino energy
R	$\mathrm{s^{-1}}$	reaction rate
X	-	parental nucleoid
Y	-	child nucleoid
Z	-	atomic number
γ	-	photon
μ	-	muon
ν	-	neutrino
ν_e	-	electron neutrino
ν_μ	-	muon neutrino
ν_τ	-	tau neutrino
τ	-	tau
Φ	$\mathrm{cm^{-2}\,s^{-1}}$	neutrino flux
σ	$\mathrm{cm^2}$	cross section

1 Introduction

1.1 The demand for sustainable mobility

In 2016 several countries agreed in the Paris Agreement to prevent a global average temperature rise higher than two centigrades above pre-industrial level. In 2018 the Intergovernmental Panel on Climate Change (IPCC) published a report stating that the limit of two degrees centigrade is not sufficiently low to prevent the Earth from harm. It requests ”rapid, far-reaching and unprecedented changes” to enforce a lower limit of 1.5 degrees centigrade [24]. The emission of green house gases, such as CO_2, needs to be reduced to minimize the global warming. Amongst other measures, power generation based on alternative energy sources has the potential to solve this problem.

Daimler AG is manufacturer of the premium car brand Mercedes and the world’s biggest manufacturer of commercial vehicles [13]. The company, as every car maker selling in the EU, has to oblige to the CO_2 emission reduction targets for passenger cars of the EU, which get stricter over time [17]. The first target of 130 grams of CO_2 per kilometer applies since 2015 and the next target of 95 grams of CO_2 per kilometer will apply in 2021. Penalties for excess emissions are issued for each car registered and are as high as €95 for each g/km of target exceedance. This results in a strong interest of Daimler in technology that allows an efficient and economic shift towards sustainable mobility.

While fueling the prevailing combustion engines with sustainable biofuels or electro-fuels can be part of this change, a major trend in the automotive sector is the shift from internal combustion engines to electric engines [23]. Sustainable technologies such as fuel cell systems or battery systems can provide the energy for these engines.

Battery electric vehicles (BEVs) constitute the largest share of the world's electric car stock, although compared to vehicles powered by internal combustion engines they lack the possibility to cover large distances without stopping to recharge [23].

Hence, technologies that extend the range of BEVs are searched for by car makers. Additional energy storage and / or energy converting systems can be added to the vehicle, such as fuel cell systems or photovoltaic panels to charge the battery while driving. However, no major breakthrough has been achieved to substitute combustion engines with a technology that can offer the same driving range at a lower price. This fact leads to the interest of the automotive industry in alternative technologies that have the ability to disrupt the current tugging war between emerging electric mobility and established combustion engines and finally give way for a future of sustainable transportation.

Sustainable transportation must be based on renewable energy sources, which can be divided into solar energy, planetary energy (gravitation) and geothermal energy. Other forms of energy are results of natural energy conversion processes [32]. To generate electricity, the part of the solar energy transmitted via photons can be used directly by photovoltaic cells. However, not all the energy released during the energy generation process in the Sun's core is released as photons; a part of it is released via neutrinos [5], making them interesting for energy conversion technologies.

1.2 Neutrinos: astronomical carriers of energy

Neutrinos are electrically neutral, very light particles that only interact via the weak force (weak interaction) and gravity [5] [36]. They do not solely originate from the Sun; other sources are nuclear reactions in the cores' of stars, astronomical events (such as the collapse of a star), natural radioactivity in the Earth's atmosphere and artificial radioactivity [5]. The existence of neutrinos was predicted by Wolfgang Pauli in 1930 and 26 years later, in 1956, experimentally confirmed by Fred Reines and Clyde L. Cowan in the Savannah River Experiment [33].

Neutrino properties and weak interactions are described in the Standard Model of particle physics, which is a quantum field theory and consists of a series of experimentally proven theories [42]. Neutrinos rarely interact with matter, which means that they can pass through the universe, including the Earth, with only a small number of interactions [5].

The fact that part of the energy released by the Sun is transmitted via neutrinos has been picked up by a company called Neutrino Deutschland GmbH. They are working on a device to harvest solar neutrinos and convert their energy into electricity [37].

The interest in neutrino harvesting technology has spread through the media, fueled by the Neutrino Deutschland GmbH [38] [10] [30] [31]. Their technology has attracted attention by hobby scientists such as Peter Lang (YouTube) [27] and other individuals such as the former German federal transport minister Günther Krause, who supported the project [18] [21].

This possibly emerging technology in the field of sustainable transportation triggered the interest of Daimler AG on its search through recently published patents. While exploring how far the interest in this concept has spread, it appears that Daimler AG is the only organization conducting research on behalf said technology. This is possibly due to the questionable functionality of such a technology.

The interest in neutrinos in astrophysical research is great. The Astroparticle Physics European Consortium (APPEC), a consortium to coordinate and fund national research efforts of its members in astroparticle physics, hopes to find answers to questions such as "What is the nature of Dark Matter and Dark Energy?" by studying neutrinos [4]. As neutrinos rarely interact with matter, they carry the valuable information about their origin through the universe [20]. Several research laboratories, such as the Laboratori Nazionali del Gran Sasso (LNGS), are or have been working on solar neutrino detectors, which convert a part of the energy carried by the neutrino into electric signals.

For the fact that neutrinos rarely interact with matter, there is no great interest in harvesting their energy. No other organization than Neutrino Deutschland GmbH and its affiliates exist that publicly pursue a strategy to harvest solar neutrinos to power electric vehicles. This idea neither has been discussed in pertinent literature. Still, with the recent activity in media around the Neutrino Deutschland GmbH and its neutrino harvesting technology, the question arises: Is it generally possible to harvest solar neutrinos for electricity generation to power electric consumers, such as cars?

1.3 Objectives

The objective of this thesis is to validate or to disprove the possibility of generating sufficient electricity to power electric cars by harvesting solar neutrinos.

The possibility of harvesting energy from solar neutrinos is analyzed in two ways:

1. Solar neutrinos are assessed on their potential as being an energy source and to supply electric consumers. To do so, the solar neutrino spectrum is analyzed and the solar neutrino energy flux is computed.
2. State-of-the-art neutrino detectors and the neutrino energy converter from the Neutrino Deutschland GmbH are analyzed on their ability to generate electricity. The neutrino interaction event rates of selected detectors are assessed and the possible output power of such detectors is calculated. The neutrino energy converter is assessed on its functionality by consulting literature.

1.4 Limitations

This study doesn't include an economical analysis of neutrino technology neither a technical feasibility study on the proposed solar neutrino energy converter as it focuses on an analysis based on science and on a state-of-the-art research.

2 Solar neutrinos

Solar neutrinos originate from the energy generation process in the Sun's core, where hydrogen nuclei merge into helium. The two fusion chains that generate solar neutrinos are the proton-proton (pp) chain, proposed by Hans A. Bethe, and the carbon-nitrogen-oxygen (CNO) cycle, proposed by Hans A. Bethe and Carl F. von Weizsäcker. The pp-chain is more likely to occur and therefore contributes to 98.4% of the solar power output [12]. The CNO-cycle is significantly less likely to occur and hence only contributes with 1.6% [40]. For this reason neutrinos from the CNO-cycle are not further contemplated in this study.

The pp-chain itself consists of several different reactions. Of these reactions only the following produce neutrinos [5]:

$$\mathrm{p} + \mathrm{p} \longrightarrow {}^{2}\mathrm{H} + \mathrm{e}^{+} + \nu_{\mathrm{e}} \qquad (q < 0.42\,\mathrm{MeV}), \tag{2.1}$$

$$\mathrm{p} + \mathrm{e}^{-} + \mathrm{p} \longrightarrow {}^{2}\mathrm{H} + \nu_{\mathrm{e}} \qquad (q = 1.44\,\mathrm{MeV}), \tag{2.2}$$

$${}^{3}\mathrm{He} + \mathrm{p} \longrightarrow {}^{4}\mathrm{He} + \mathrm{e}^{+} + \nu_{\mathrm{e}} \qquad (q < 18.8\,\mathrm{MeV}), \tag{2.3}$$

$${}^{7}\mathrm{Be} + \mathrm{e}^{-} \longrightarrow {}^{7}\mathrm{Li} + \nu_{\mathrm{e}} \qquad (q = 0.86\,\mathrm{MeV}\ (90\%), 0.38\,\mathrm{MeV}\ (10\%)), \tag{2.4}$$

$${}^{8}\mathrm{B} \longrightarrow {}^{8}\mathrm{Be}^{*} + \mathrm{e}^{+} + \nu_{\mathrm{e}} \qquad (q < 15\,\mathrm{MeV}). \tag{2.5}$$

Energy, measured in electronvolts (eV), is released in these reactions and carried away by the produced particles as kinetic energy. One electronvolt is defined as $1\,\mathrm{eV} = 1.602\,176\,634 \times 10^{-19}\,\mathrm{J}$ and equal to the energy of an electron accelerated by an electric field in vacuum by a voltage of one volt. The energy released as neutrino energy (q) is given for each reaction.

Solar neutrinos are named after the reaction that produce them: pp, pep, hep, ^{7}Be and ^{8}B respectively. They are referred to as neutrino branches in this study.

The pp-reaction is the fusion process of two protons (p) into a nucleus of deuterium (^{2}H) under the emission of a positron (e^{+}), which is the antiparticle of the electron, and an electron neutrino (ν_e). The neutrinos (pp-neutrinos) emitted by this process possess an energy below 0.42 MeV with an average energy of ~ 0.265 MeV [39]. The largest amount of solar neutrinos (pp-neutrinos) is coming from this reaction, which constitutes roughly 91% of the solar neutrino output [5]. The ^{7}Be-neutrinos make up about 7% of the solar neutrino generation. They are produced, when a beryllium atom (^{7}Be) captures an electron and transforms into a lithium atom (^{7}Li) with the emission of an electron neutrino (^{7}Be-neutrino). This reaction releases neutrinos only at two discrete energies: $q = 0.86$ MeV with a probability of 90% and $q = 0.38$ MeV with a probability of 10%. The numbers of neutrinos produced by the pep, hep and ^{8}B-reactions are small compared to the other sources. The neutrinos produced by the pep-reaction are monochromatic with an energy of 1.44 MeV. The hep-reaction produces neutrinos with the lowest flux but with the highest energy for solar neutrinos: they range below 18.8 MeV. Neutrinos coming from the ^{8}B-reaction range below 15.5 MeV.

The standard solar model gives a mathematical description of the neutrino creation process in the Sun and is able to predict resulting solar neutrino fluxes (Φ) on the Earth's surface (see Table 2.1). The neutrino fluxes are given in number of incident neutrinos per cm^2 per second.

Table 2.1: Solar neutrino fluxes with uncertainties as calculated by John N. Bahcall [5].

Source	Φ (10^{10} cm^{-2} s^{-1})
pp	$6.0\ (1 \pm 0.02)$
pep	$0.014\ (1 \pm 0.05)$
hep	8×10^{-7}
^{7}Be	$0.47\ (1 \pm 0.15)$
^{8}B	$5.8 \times 10^{-4}\ (1 \pm 0.37)$

The neutrino energies of the fluxes have a spectral distribution, shown in Figure 2.1. In the neutrino spectrum, the units for the continuum (spectral) fluxes λ are given in number of incident neutrinos per cm^2 per second per MeV and the units for discrete energy fluxes Φ, such as ^{7}Be, are given in number of incident neutrinos per cm^2 per second.

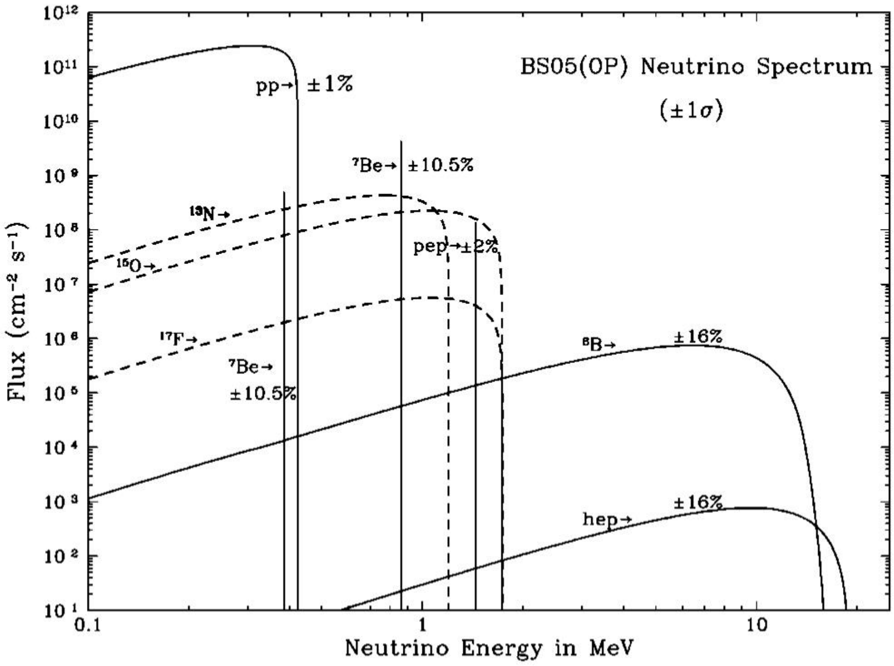

Figure 2.1: Solar neutrino spectrum for the solar model BS05(OP) [5]. The units for the continuum (spectral) fluxes λ are number of incident neutrinos per cm^2 per second per MeV and the units for discrete energy neutrino fluxes Φ, such as ^7Be, are number of incident neutrinos per cm^2 per second. The uncertainties are taken from Table 8 of Bahcall & Serenelli [6].

From now on, the combination of the standard solar model and the Standard Model of particle physics is simply referred to as standard model in this study.

Electron neutrinos (ν_e) emitted by the Sun, once they reach the Earth, undergo two fundamentally different interactions with matter:

- neutrino capture, where a neutrino is absorbed by an atomic nucleus,
- neutrino scattering, where a neutrino scatters with an electron or atomic nucleus.

How these interactions are used to detect solar neutrinos is explained in section 3.1.

Besides electron neutrinos, other so called neutrino flavors exist: muon neutrinos (ν_μ)

and tau neutrinos (ν_τ). They are named after the heavier siblings of the electron, which are the muon (μ^-) and the tau (τ^-). Neutrinos of no specific flavor are denoted as ν_x.

Even though the Sun only emits electron neutrinos, not all solar neutrinos reaching the Earth are of this flavor. This fact was discovered by Raymond Davis and John N. Bahcall in the Homestake experiment and explained by the theory of neutrino oscillations. This theory describes how neutrinos can change flavors while traveling through space and got validated by the Sudbury Neutrino Observatory (SNO) in 2001.

In this study, neutrino oscillations are neglected for reasons of simplicity and calculations are performed based on the solar neutrino flux predicted by the standard model.

3 State-of-the-art solar neutrino technology

This chapter gives an overview of the existing neutrino technology, including neutrino detectors and a neutrino energy converter. While neutrino detectors focus on accurate measurements of neutrino properties, converters strive to maximize the energy conversion rate from neutrino energy to electricity. Only one technology in the field of neutrino energy converters has been found and is treated in section 3.2.

3.1 Solar neutrino detectors

Solar neutrino detectors allow the measurement of solar neutrino fluxes, based on the interaction of incoming neutrinos with the detector material. In the detectors, a target, such as a nucleus or an electron, is exposed to a neutrino flux (Φ), which leads to an interaction rate (R), measured in number of interactions per unit time per target.

For the absorption of solar neutrinos by nuclei, the interaction rate R is usually given in solar neutrino units (SNUs) [5]; for convenience a SNU is defined as:

$$1\,\mathrm{SNU} = 10^{-36}\,\mathrm{s}^{-1}. \tag{3.1}$$

The amount of neutrino interactions with a target exposed to a neutrino flux Φ depends on the cross section σ of the interaction (given in cm^2). It can bee seen as the apparent target area for incoming neutrinos and is defined as

$$\sigma = \frac{R}{\Phi}. \tag{3.2}$$

The standard model allows the calculation of cross sections for individual neutrino interactions. Larger cross sections are expected to yield a larger amount of interactions. Compared to the interactions of other particles via the strong or electromagnetic force, neutrino interaction cross sections are several orders of magnitude lower [7]. For example, the capture of a neutron by a target nucleus, lies in the order of $10^{-24}\,\mathrm{cm}^2$.

Table 3.1 shows neutrino absorption reactions of ^{37}Cl and ^{71}Ga, which are used in some of the presented neutrino detectors.

Table 3.1: Neutrino absorption cross sections averaged over energy spectra, as calculated by J. N. Bahcall [5]. The units for pp, pep and ^{7}Be-neutrinos are given in $10^{-46}\,\mathrm{cm}^2$, while for hep and ^{8}B-neutrinos they are given in $10^{-42}\,\mathrm{cm}^2$.

Target	pp	pep	hep	^{7}Be	^{8}B
^{37}Cl	0.0	16	3.9	2.4	1.06
^{71}Ga	11.8	215	7.3	73.2	2.43

The cross sections for neutrino absorption in ^{71}Ga are larger than in ^{37}Cl, which results in a higher number of interactions per target nucleus. The cross section for pp-neutrinos with the chlorine target is zero, which means that no interactions are expected.

Cross sections of neutrino-electron scattering events for the different branches of solar neutrinos are shown in Table 3.2.

Table 3.2: Neutrino-electron scattering cross sections, as calculated by J. N. Bahcall [5]. The neutrino energy (q) and the maximum electron recoil energy ($T_{\max}$) are given in MeV. The neutrino-electron scattering cross section ($\sigma_{\nu_e - e}$) is given in units of $10^{-46}\,\mathrm{cm}^2$.

Source	q	$T_{\max}$	$\sigma_{\nu_e - e}$
pp	≤ 0.420	0.261	11.6
pep	1.442	1.225	112
hep	≤ 18.773	18.52	884
^{7}Be	0.862	0.665	59.3
^{7}Be	0.384	0.231	19.6
^{8}B	≤ 15.0	14.5	608

The maximum electron recoil energies lie below the neutrino energies, as only a part of the neutrino energy is transferred in the scattering event. The lowest neutrino-electron scattering cross section is obtained for pp-neutrinos, while the hep-neutrinos show the largest cross section.

Different types of detectors were designed to measure neutrino interactions. Table 3.3 gives an overview of the presented solar neutrino detectors in this section. They were selected because of their importance in solar neutrino research.

Table 3.3: List of selected solar neutrino experiments sorted by their operating time.

Name	Type	Operating time
Homestake Experiment	Radiochemical	1970 - 1994
Kamiokande-II	Water Cherenkov	1985 - 1990
GALLEX & GNO	Radiochemical	1991 - 2002
SuperKamiokande	Water Cherenkov	1996 - 2001
SNO	Water Cherenkov	1999 - 2006
Borexino	Scintillator	Since 2007
DARWIN	Scintillator, TPC	planned (undefined)

The Homestake experiment and the two gallium experiments (GALLEX & GNO) have been radiochemical detectors. Three water Cherenkov detectors are described in this study: Kamiokande-II, its successor SuperKamiokande and SNO. Finally, scintillation detectors are described, of which Borexino is still running and DARWIN is not yet constructed.

In radiochemical detectors, neutrino interactions produce unstable nuclei, which decay over time. After some time of exposure to the solar neutrino flux, the unstable nuclei can be extracted from the detector. Measuring their decay rate allows to draw conclusions on the neutrino interaction.

In neutrino detectors such as scintillation counters, Cherenkov counters and time projection chambers (TPCs) the neutrino interactions finally lead to light emission, which is measured by photomultiplier (PMT) arrays. The properties of the measured light give insight into the neutrino interactions.

3.1.1 Radiochemical detectors

In radiochemical detectors, target nuclei exposed to a solar neutrino flux capture neutrinos at the rate R. The neutrino capture leads to the decay of a parental nucleus X and produces an unstable child nucleus Y under the emission of an electron (e^-):

$$\nu_e + {}^{A}_{Z}X \longrightarrow {}^{A}_{Z+1}Y + e^-. \tag{3.3}$$

This process is known as beta decay, with A being the mass number and Z the atomic number.

After some time passed, the unstable nuclei can be extracted from the detector and their decay rates can be measured. For this measurement gas detectors, such as the proportional counter, are used.

Three of the presented detectors fall into this category: the Homestake experiment and the gallium detectors GALLEX & GNO.

The Homestake experiment

The first experiment to detect solar neutrinos was conducted by Raymond Davis and John N. Bahcall in the late 60's using a radiochemical detector based in the Homestake mine in South Dakota. They started building the detector in 1965, which was completed four years later. It took first data in 1970 and ran until the early 1990s. The detector was filled with 615 tons of liquid tetrachloroethylene (C_2Cl_4).

When a chlorine nucleus (^{37}Cl) captures a neutrino, it decays into a radioactive argon nucleus (^{37}Ar) and emits an electron:

$$^{37}\mathrm{Cl} + \nu_e \longrightarrow {}^{37}\mathrm{Ar} + e^- . \tag{3.4}$$

During the runtime of the experiment, the produced argon was extracted every two months by forcing helium through the liquid. The argon core ^{37}Ar is unstable and decays with a half-life of 35 days. This decay is measured with proportional counters in order to draw conclusions about the precedent neutrino interactions [12].

The detector could only detect neutrinos from the ^7Be and ^8B branches, as the threshold energy E_{th} for reaction 3.4 ranges at $\sim 0.8\,\mathrm{MeV}$ [5]. The threshold energy is the minimal kinetic energy the incoming particles must have to undergo the interaction. As the chlorine core is considered at rest the threshold energy is brought up by the neutrino alone.

The gallium detectors: GALLEX and GNO

Other examples are the GALLEX (GALLium EXperiment) and GNO (Gallium Neutrino Observatory) projects. They were designed to look out for solar neutrinos from the pp-branch. GALLEX was a radiochemical experiment located in the Laboratori Nazionali del Gran Sasso (LNGS) in Italy [25]. It was conducted by a research cooperation lead by the Max Planck Institute for Nuclear Physics (MPIK) Heidelberg. The neutrino target is comprised by 30.3 t gallium as part of a concentrated $GaCl_3$-HCl solution with a total weight of 101 t. Figure 3.1 shows the tank with the solution and the absorption system.

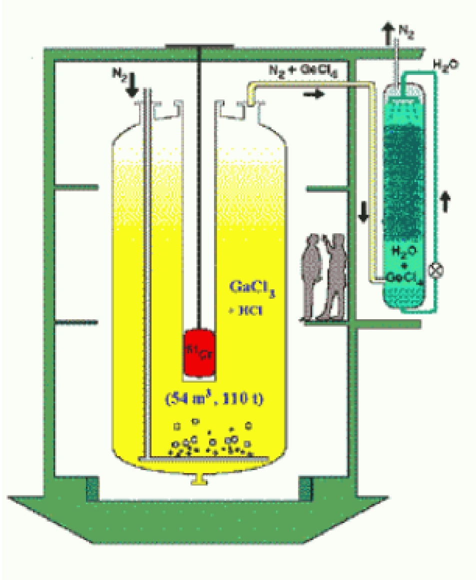

Figure 3.1: Scheme of the GALLEX detector tank. Inside the tank with the gallium target solution, a chromium source can be placed for calibration reasons. The tank on the right hand side represents the absorber system to extract the produced germanium [25].

When a gallium nucleus (^{71}Ga) captures a neutrino it decays according to the following beta decay process:

$$\nu_e + {}^{71}\mathrm{Ga} \longrightarrow {}^{71}\mathrm{Ge} + e^- \tag{3.5}$$

During the decay ^{71}Ga captures an electron neutrino and transforms into radioactive germanium (^{71}Ge) under the emission of an electron. After three or more weeks of neutrino interactions with the target, the tank is purged with nitrogen to remove the germanium. Proportional counters are used to measure the decay rates of germanium, which can be related to the neutrino interactions [25].

With a threshold energy of $E_{\mathrm{th}} = 233\,\mathrm{keV}$, the experiment was able to detect solar neutrinos with relatively low energies, such as pp-neutrinos. Data was taken from 1991 to 1997.

Finally, GALLEX was succeeded by GNO, which used the same 30 t gallium target and the same neutrino absorption process, while the accuracy was refined and the operation simplified. GNO took data from 1998 until 2002.

3.1.2 Water Cherenkov technique

Water Cherenkov detectors use Cherenkov radiation to detect neutrinos. Cherenkov radiation is emitted by charged particles traversing a medium faster than the phase velocity of light. It can be referred to as the optical analogous to the sonic boom for sound waves. Figure 3.2 visualizes the process of Cherenkov light generation. The emitted light is detected by PMTs via the photoelectric effect, converting the kinetic energy of the photons into electricity.

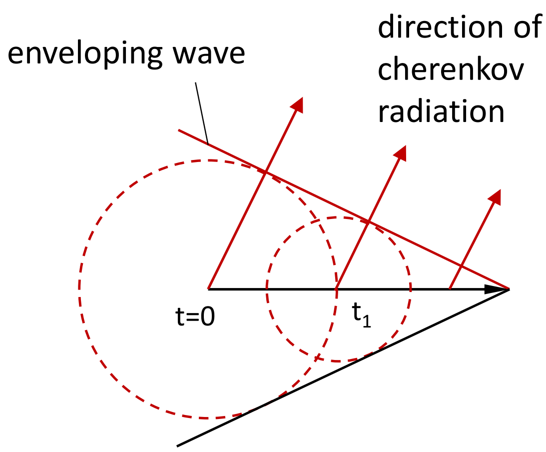

Figure 3.2: Cherenkov radiation emitted from a particle traversing faster than light through a medium. The radiation intensifies in one direction, where it can be detected [15].

Several detectors are based on this working principle, amongst them are: Kamiokande II & SuperKamiokande and the Sudbury Neutrino Observatory.

Kamiokande II and SuperKamiokande

Kamiokande II and SuperKamiokande are based on the water Cherenkov technique and located 1,000 meters underground in the Kamioka-mine, Hida-city, Gifu, Japan. The Kamiokande detector consists of 3,000 tons of water surrounded by 1,000 PMTs, while

SuperKamiokande is a bigger version with 50,000 tons of water and 11,200 PMTs. The detection mechanism is based on neutrino-electron scattering:

$$\nu_e + e^- \longrightarrow \nu_e + e^-, \tag{3.6}$$

where a variable amount of kinetic energy is transferred from the neutrino to the electron and leads to the recoil of the electron [28]. The recoiling electron produces Cherenkov light, which is captured by PMTs.

This technique allows neutrino detection with a threshold energy of $E_{th} = 7.5$ MeV for Kamiokande and $E_{th} = 5.5$ MeV for SuperKamiokande, which makes the detectors suitable mostly for the detection of the ^{8}B and hep-neutrinos [29].

Sudbury Neutrino Observatory (SNO)

The Sudbury Neutrino Observatory (SNO) was built to detect ^{8}B neutrinos and located 6,010 meters below sea level near Sudbury, Ontario, Canada. It consisted of a tank filled with 1,000 tons of deuterium oxide (^2H_2O), also known as heavy water. The observatory was equipped with PMTs to detect the emitted Cherenkov light. With a threshold energy of 3.5 MeV the detector achieved the lowest neutrino threshold energy for water Cherenkov detectors [8]. The SNO took data from 1999 until 2006

The SNO makes use of three neutrino interactions (3.7, 3.8 and 3.9) to detect solar neutrinos [5]. All of the reactions are followed by the emission of Cherenkov light, which is captured by the PMTs and gives information about the neutrino event. Two interactions involve the core of the deuterium target, which is referred to as deuteron (d):

$$\nu_e + d \longrightarrow p + p + e^-, \tag{3.7}$$

where deuteron absorbes an electron neutrino and decays, under the emission of an electron, into two protons, and

$$\nu_x + d \longrightarrow p + n + \nu_x \qquad (x = e, \mu, \tau), \tag{3.8}$$

where deuteron interacts with a neutrino and disintegrates. The third interaction is a neutrino-electron scattering process:

$$\nu_x + e^- \longrightarrow \nu_x + e^- \qquad (x = e, \mu, \tau). \tag{3.9}$$

3.1.3 Scintillation detectors

In a scintillation detector, light is produced from charged particles traversing a transparent scintillation medium that re-emits absorbed energy as gamma rays. The scintillation medium can be in solid, liquid or gaseous state.

The working principle of a scintillation detector for solar neutrinos can be explained as follows [15]:

1. Incident neutrinos cause recoiling electrons in the hull of atoms, which constitute the scintillation medium.
2. The recoiling electrons excite neighboring atoms.
3. In a deexcitation process the excited atoms emit photons, which are detected with the aid of photomultipliers (PMTs).
4. Time, location and energy of the photon emissions are analyzed and give information about the neutrino interaction.

In the following, selected detectors are presented, which are based on this working mechanism: Borexino and DARWIN. While Borexino is currently running and taking data, DARWIN is still in the planning stage.

Borexino: the boron experiment

Up to now, the Borexino detector is the only scintillation experiment used to detect solar neutrinos. Its target material is based on boron (B); hence the name: Borexino is the Italian diminutive of BOREX (BORon solar neutrino EXperiment). As the gallium experiments from section 3.1.1, it is located in the LNGS in Italy approximately 3800 meters underneath the sea level. This location allows measurements with a low background, as the rock cover protects the detector from radiation. At present, the interior of the Borexino detector shows the least radioactivity of all places in the world [26]. It has a relatively low threshold energy for neutrino interactions with $E_{\text{th}} \approx 150\,\text{keV}$ [9] and is designed to measure the flux of incoming solar ^{7}Be neutrinos [29]. The detector (see Figure 3.3) consists of a stainless steel sphere with a radius of 6.85 m, shielded by an external water tank. The sphere contains a buffer medium and the scintillator liquid. Internal PMTs measure the light signals from the scintillating liquid while external PMTs measure background flux in the water. The region of the detector where the background is reduced sufficiently and which is used to detect the desired neutrino signal, is referred to as fiducial volume. In the Borexino detector, the liquid scintillator that constitutes the fiducial volume weighs 100 t [2].

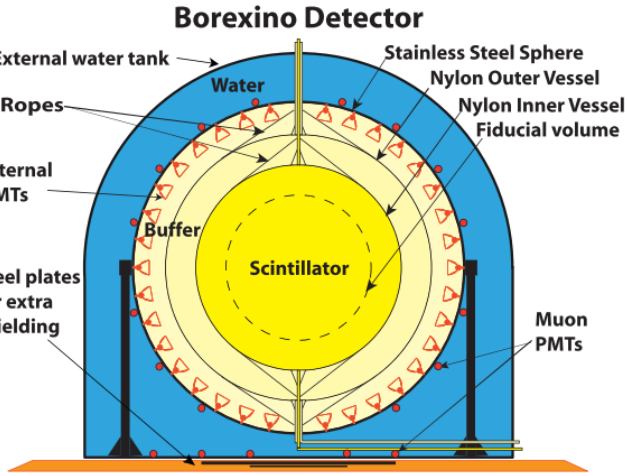

Figure 3.3: Cross-section through the Borexino detector. The nylon inner vessel in the center contains the scintillator liquid. It is surrounded by a buffer contained in a stainless steel sphere. The nylon vessels are suspended by ropes. The internal PMTs are situated inside the stainless steel sphere to detect the neutrino interactions. The steel sphere is contained in an external water tank where outer PMTs are placed to track the muon activities [2].

The scintillation liquid consists of a solvent and a solute: the solvent is a pseudocumene (PC) 1,2,4-trimethylbenzene ($C_6H_3(CH_3)_3$) and the solute is the fluor PPO 2,5-diphenyloxazole ($C_{15}H_{11}NO$). The concentration is 0.17% by weight [2]. This PC/PPO solution allows solar electron neutrino detection via neutrino-electron scattering $\nu_e + e^- \longrightarrow \nu_e + e^-$ [2]. The recoil energy of the electron leads to photon emission due to scintillation. The light is collected by 2212 PMTs evenly distributed inside the stainless steel sphere [2].

DARWIN

DARWIN (DARk matter WImp search with liquid xenoN) is a planned experiment, which amongst other research goals, aims to detect solar neutrinos from the pp and ^{7}Be-branches [1]. The hosting laboratory and the start of construction for the experiment are still undefined [41].

Similar to Borexino, DARWIN uses the light signals of scintillation to detect neutrinos, but its measurement system is more complex: it is designed as a time projection chamber.

A time projection chamber uses a scintillator medium and PMTs to detect incoming neutrinos. After an incoming neutrino has interacted with the target material, recoiling electrons are further accelerated by an electrical field applied to the chamber. This results in two subsequent light signals, which are captured by the PMTs.

As target material, DARWIN works with 50 t of liquid xenon, with the fiducial region accounting for 30 t. For the detection of pp-neutrinos the neutrino-electron scattering reaction $\nu_e + e^- \longrightarrow \nu_e + e^-$ is used. A threshold of 1 keV is expected [35].

3.2 Solar neutrino energy converters

The only neutrino energy converter published is a device by Neutrino Deutschland GmbH. It is an invention of its CEO, Holger Thorsten Schubart, and has been filed for patent in 2015 with the number WO2016142056A1 [37]. The patent describes the energy converter and outlines its manufacturing process.

The proposed energy converter consists of a composite structure: a metallic base material is coated with one or more semiconductor materials and graphene. The coating (or the uppermost layer thereof) acts as the anode of the device meanwhile the base acts as the cathode. The patent explains that an electric current flows once the electrodes are connected to a load. Figure 3.4 visualizes the description given in the patent.

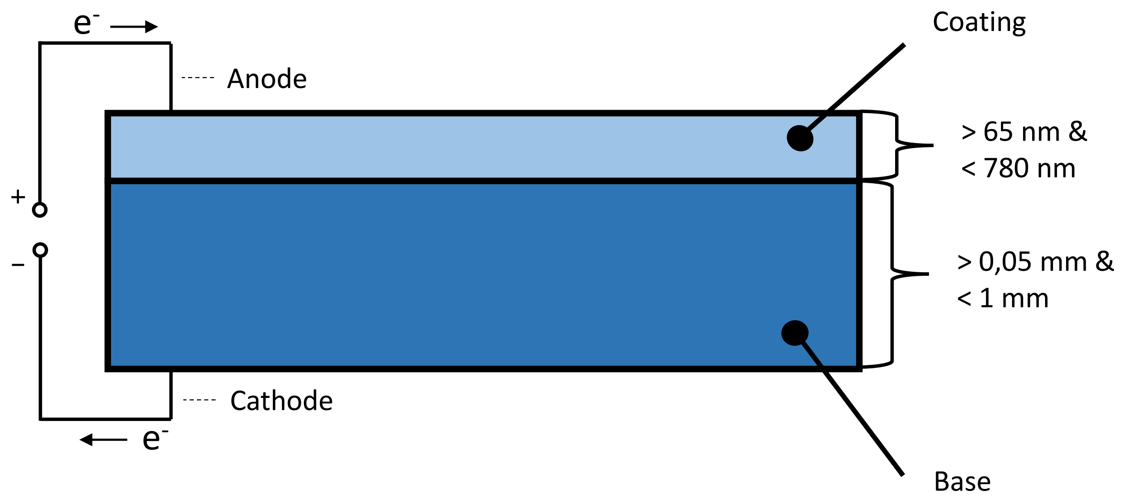

Figure 3.4: Scheme of the invention described in the patent. The lower part is the base and includes a connector. The base is coated with a mix of 25% silicon and 75% graphene.

The base is comprised by a metal foil. As stated by the patent, the following metals can be used as foil materials: silver, gold, copper, gallium or aluminum. According to the patent, using silver as base material achieves the best performance because of its high electric conductivity. An ideal thickness of the foil t_{foil} is indicated as $0.05\text{ mm} <= t_{\text{foil}} <= 1\text{ mm}$.

The base is ideally coated with 75% graphene and 25% silicon. According to the patent, the energy conversion efficiency increases with shrinking graphene particle size, where ideally, a particle size of 20 nm is achieved. For the silicon, a particle size of 5 nm is optimal. The coating can either be a mixture or separate layers, with separate layers leading to better results. Ideally, coatings have alternating layers of silicon and graphene, where 12 silicon-graphene-layers are given as an optimum (see Figure 3.5).

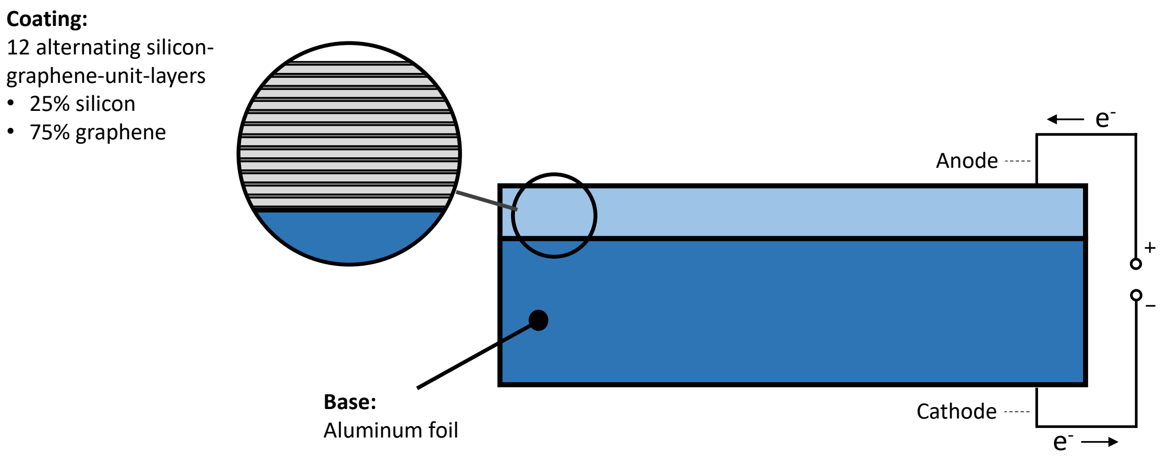

Figure 3.5: Schematic of the neutrino energy converter with multilayer coating on an aluminum base. The coating consists of 12 alternating silicon-graphene-unit-layers.

By stacking three particles of graphene and one of silicon on top of each other to achieve the 1:3 ratio, the coating must have a minimal thickness of approximately 65 nm. The upper value for the thickness, which can be obtained by calculating the case for a 12-layered configuration, is 780 nm.

According to the patent, the lattice structure of the coating is nanotechnologically modified. This is achieved partly by the deposition process and partly by doping the graphene. The patent gives the following dopant candidates for doping: ferroniobium, nickelniobium, yttrium and samatrium oxide. The so modified graphene, as stated in the patent, decelerates the incoming neutrinos at around 0.1‰ and transfers some of their kinetic energy in a "pendulum movement" to the silicon layer and then to the base.

Up to now, no prototype of this invention has been presented to the public.

4 Methodology

The work plan of this research is given in three steps:

1. An electric passenger car is exemplarily chosen to estimate the power need of an electric vehicle of Daimler AG. This provides the base for further evaluations regarding the question if its energy needs can be met by harvesting solar neutrinos.
2. The energy inherent to the solar neutrino flux on the Earth's surface is calculated.
3. The state-of-the-art neutrino technology, including detectors and the one converter, are analyzed.

4.1 Energy need of electric vehicles

To give an estimation of the energy which needs to be harvested from solar neutrinos to power electric vehicles, the passenger car Mercedes-Benz EQC is taken into consideration [19]. The Mercedenz-Benz EQC is chosen, as it is the first BEV of the electric car brand EQ by Daimler AG. According to the electric vehicle data base [16], the Mercedenz-Benz EQC has a usable battery capacity of 80 kWh and a real range of 322 km (200 miles). If one chooses to charge the battery within 10 h, a permanent power of 8 kW is needed. This is an assumption to design a potential neutrino energy converter and not related to conventional charging facilities of the car. The dimensions of the car are 4.76 m (length) times 1.88 m (width) [16], leading to a surface area of 8.97 m^2.

4.2 Energy flux through neutrino irradiation

This section introduces a method to calculate the solar neutrino energy flux (P_ν), given in W/m^2, resulting from solar neutrino irradiation on the Earth's surface. Here, neutrino interactions with the atmosphere are neglected.

The solar neutrino energy flux can be calculated based on the solar neutrino spectrum (see Figure 2.1 in chapter 2), which shows six continua and two discrete branches. The neutrinos coming from the CNO-cycle are disregarded, as their energies and fluxes are relatively low. This leaves us with three continua (pp, ^{8}B and hep) and two discrete branches (^{7}Be and pep). The data of the continua is extracted from Figure 2.1 via the tool WebPlotDigitizer [34] and displayed in Figure 4.1. The fluxes and neutrino energies for the discrete energy branches can be taken directly from Bahcall [5].

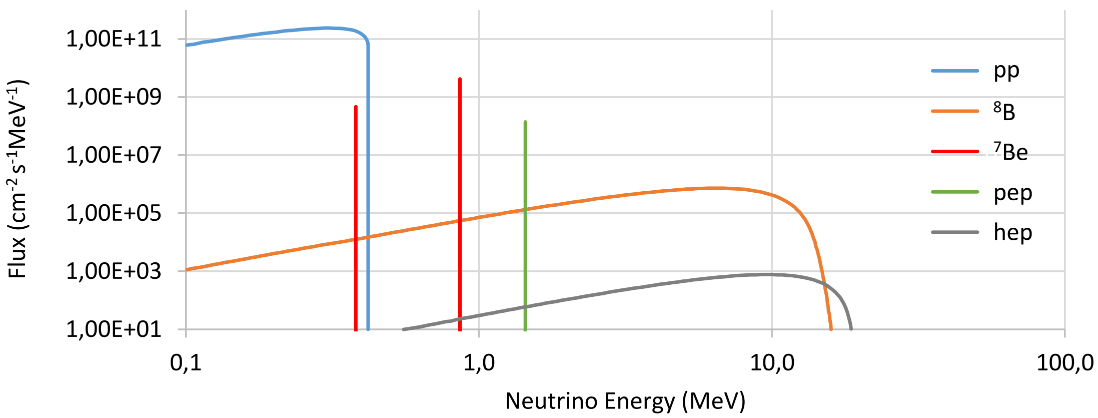

Figure 4.1: The values for the continua of the pp-chain are obtained via the tool WebPlotDigitizer [34]. The fluxes of the discrete neutrino branches are taken from Bahcall [5].

To obtain the branch energy fluxes P_b in $\text{MeV}\,\text{cm}^{-2}\,\text{s}^{-1}$, the discrete fluxes $\Phi_{^7\text{Be}}$ and Φ_{pep}, given in $\text{cm}^{-2}\,\text{s}^{-1}$, need to be multiplied with the corresponding neutrino energy q. The subscript b denotes the neutrino branch. The pep-neutrinos are emitted at a single energy q_{pep} and their energy flux P_{pep} can be calculated with:

$$P_{\mathrm{pep}} = \Phi_{\mathrm{pep}} \times q_{\mathrm{pep}}. \tag{4.1}$$

Neutrinos from the ^{7}Be-branch are emitted at two discrete energies with different probabilities resulting in two fluxes. For this reason, the individual ^{7}Be-fluxes need to be multiplied with the corresponding neutrino energy and summed up. The equation can be written as:

$$P_b = \Phi_{b,1} \times q_{b,1} + \Phi_{b,2} \times q_{b,2} \qquad \text{for } b = {}^7\mathrm{Be}. \tag{4.2}$$

The energy flux for the continua is calculated based on the neutrino spectra $\lambda_{\mathrm{pp}}(q)$, $\lambda_{^8\mathrm{B}}(q)$ and $\lambda_{\mathrm{hep}}(q)$, which are given in $\mathrm{cm^{-2}\,s^{-1}\,MeV^{-1}}$. They need to be integrated twice to yield the energy fluxes P_b of the individual branches. The calculation to be performed is:

$$P_b = \iint \lambda_b(q)\, dq\, dq \qquad \text{for } b = \mathrm{pp},\ {}^8\mathrm{B},\ \mathrm{hep}. \tag{4.3}$$

Integrations are performed for each neutrino branch individually, where the respective minimal and maximal neutrino energies represent the integration boundaries (see Table 4.1). Hereby, values for neutrino energies below 0.1 MeV, as well as fluxes under 10 $\mathrm{cm^{-2}\,s^{-1}}$, are disregarded.

Table 4.1: The integration boundaries, given in MeV, are listed for the neutrino branches pp, hep and ^{8}B.

Neutrino branch	Lower boundary	Upper boundary
pp	0.101	0.419
hep	0.553	18.640
^{8}B	0.100	15.920

To perform the numerical integration, the trapezoidal rule with a varying step width depending on the raw data is chosen as integration method.

Finally, the sum of the energy fluxes of all branches is the total solar neutrino energy flux P_ν expected on Earth's surface.

4.3 Analysis of the state-of-the-art

The presented solar neutrino detectors and the solar neutrino energy converter are assessed on their ability to generate electricity by harvesting the energy of solar neutrinos. For selected detectors, the neutrino interaction event rate is studied and the power output is estimated. For the neutrino converter, graphene and doped graphene are assessed on their neutrino harvesting abilities by consulting literature. To do so, the threshold energy of graphene is compared to the energies of the solar neutrino branches.

4.3.1 Analysis of solar neutrino detectors

At first, the detectors presented in this section are analyzed on their neutrino detection capability. At second, to calculate the power output, two detectors which are capable of detecting the high fluxes of pp- and ^{7}Be-neutrinos are chosen: GALLEX and DARWIN.

GALLEX

In GALLEX the reaction $\nu_e + {}^{71}\mathrm{Ga} \longrightarrow {}^{71}\mathrm{Ge} + e^-$ takes place, where a neutrino is captured by a gallium nucleus. The standard model allows to predict neutrino capture rates of ^{71}Ga for all neutrino branches, resulting in 70.8 SNU for pp-neutrinos and 34.3 SNU for ^{7}Be-neutrinos [5]. In the 30 t ^{71}Ga-target of GALLEX, this leads to 0.63 events per day for pp-neutrinos and to 0.30 events per day for ^{7}Be-neutrinos (see Table 4.2) [5].

Table 4.2: Neutrino capture and event rates for chosen neutrino branches in GALLEX. The neutrino capture rate is given in SNU and the event rate is given in number of events per day [5].

Neutrino branch	Capture rate	Event rate
pp	70.8	0.63
^{7}Be	34.3	0.30

Two assumptions are taken:

1. The neutrino energy is fully absorbed in the reaction $\nu_e + {}^{71}\text{Ga} \longrightarrow {}^{71}\text{Ge} + e^-$.
2. No energy losses occur in the detector.

Then, the power output of the detector P_{detector} measured in watts can be calculated by multiplying the corresponding daily event rates with the average energy of the pp and ^{7}Be-neutrinos respectively and with a conversion factor ($\frac{\text{day}}{86\,400\,\text{s}}$):

$$P_{\text{detector}} = \{\text{daily event rate}\}_x \times q_{x,\text{avg}} \times \frac{\text{day}}{86\,400\,\text{s}} \qquad \text{for } x = \text{pp}, {}^7\text{Be}. \tag{4.4}$$

The average energy of ^{7}Be-neutrinos $q_{^7\text{Be,avg}}$ can be calculated with the probabilities and corresponding neutrino energies given in reaction 2.4 in chapter 2 as:

$$q_{^7\text{Be,avg}} = 0.86\,\text{MeV} \times 0.9 + 0.38\,\text{MeV} \times 0.1. \tag{4.5}$$

Finally the specific power P' in watts per tonne can be obtained by dividing the power output by the detector material weight.

DARWIN

In DARWIN incident solar neutrinos lead to electron recoils, which in turn lead to the production of scintillation light. This scintillation light is captured by PMTs, where it is converted into electricity. For calculating the power output, it is assumed that the conversion of electron recoil energy to electricity is ideal (no energy losses occur).

Aalbers et al. [1] calculated the electron recoil energy for a neutrino-electron scattering event in the xenon target of DARWIN (see Figure 4.2).

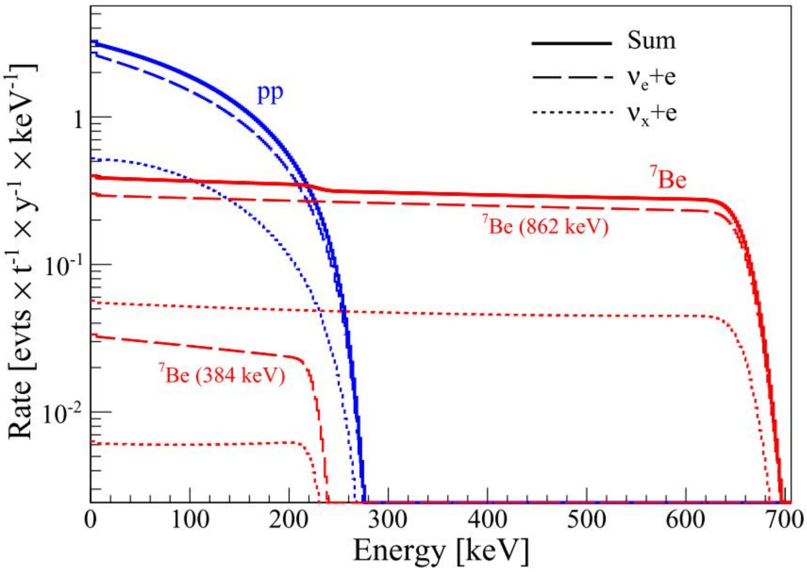

Figure 4.2: Differential electron recoil spectra in liquid xenon [1]. The interaction rate in events per tonne per year per keV (evts t^{-1} y^{-1} keV^{-1}) is plotted against the neutrino energy in keV.

To obtain the specific power P' in W/t from the data, two integration rounds need to be performed. The data to base these calculations on is obtained via WebPlotDigitizer [34] from Figure 4.2. The chosen integration method is the trapezoidal rule with a varying step width, depending on the raw data. After the first round, the data will have the unit evts t^{-1} y^{-1} and after the second integration the specific power in keV t^{-1} y^{-1} is obtained. Manipulating the data leads to the specific power P' in W/t.

4.3.2 Analysis of the neutrino energy converter

The converter described in the patent uses doped graphene to harvest neutrinos. Two methods are used to assess its abilities to harvest solar neutrinos:

1. Literature is consulted to assess the interaction between carbon atoms and solar neutrinos.
2. An analysis showing the effects of doping on the device's neutrino harvesting abilities is performed.

5 Results

5.1 Results from calculation of the energy flux through neutrino irradiation

This section presents the results from the calculation of the energy flux through neutrino irradiation. For the continuum spectra (pp, hep and ^{8}B) two integrations are performed. After the first integration, the neutrino fluxes in incident neutrinos per cm^2 per second are obtained and compared with values from literature [5] to assess the accuracy of the data (see Table 5.1). All deviations lie under 7%.

Table 5.1: The calculated neutrino fluxes of the continuum energy branches (pp, hep and ^{8}B) are shown and compared to reference values calculated by John N. Bahcall [5].

Neutrino branch	Flux ($\mathrm{cm^{-2}\,s^{-1}}$)	Reference flux ($\mathrm{cm^{-2}\,s^{-1}}$)	Deviation in %
pp	5.61×10^{10}	6.00×10^{10}	6.48
hep	7.97×10^{3}	8.00×10^{3}	5.04
^{8}B	5.51×10^{6}	5.80×10^{6}	0.36

The next integration step leads to the neutrino energy fluxes of the individual branches with units of $\mathrm{MeV\,cm^{-2}\,s^{-1}}$. This data, together with the calculated energy fluxes of the discrete branches (^{7}Be and pep), is presented in Table 5.2.

Table 5.2: The energy fluxes obtained from the different solar neutrino branches are listed.

Neutrino source	energy flux (W/m^2)
pp	12.96
pep	0.21
hep	1.15×10^{-4}
^{7}Be	6.12
^{8}B	8.10×10^{-2}
Sum	19.49

The energy flux from pp-neutrinos represents the largest share, followed by the ^{7}Be neutrinos. The other neutrino branches can be neglected as they contribute only little to the energy flux. Summing up the solar neutrino energy fluxes results in $P_\nu = 19.49\,W/m^2$.

Due to the low interaction probabilities of neutrinos with matter (low cross sections), only a tiny fraction of this energy can potentially be used. Even when considering that the flux could be fully absorbed, a surface of $\sim 400\,m^2$ is needed to deliver the required power of 8 kW to charge the battery of the Mercedes-Benz EQC in 10 h. This surface exceeds the surface of the car, which is below $10\,m^2$, by far. Therefore, it is not possible to power electric vehicles by harvesting solar neutrinos.

5.2 Results from analysis of the state-of-the-art

5.2.1 Results from analysis of solar neutrino detectors

Contemplating the solar neutrino detectors listed in the state-of-the-art, research shows that a large amount of target material is needed to capture signals from incoming neutrinos. Table 5.3 shows the weight of the target material used.

Table 5.3: The detectors, which where presented earlier are listed with their target material weight (m_t).

Name	m_t in tonnes
Homestake Experiment	615
Kamiokande-II	3000
GALLEX & GNO	101
SuperKamiokande	50000
SNO	1000
Borexino	100
DARWIN	50

Neutrinos of the pp and ^{7}Be-branches account for the highest energy fluxes, as calculated in section 5.1. However, as the energies carried by a single neutrino are relatively low (below 0.4 MeV), only few detectors have sufficiently low threshold energies to detect them. Table 5.4 lists the analyzed detectors with their respective threshold energies for neutrino interactions. Amongst the detectors that are able to detect these low energies are SNO, GALLEX, GNO, Borexino and DARWIN.

Table 5.4: The detectors, which where presented earlier are listed with their neutrino detection threshold energies (E_{th}).

Name	E_{th} in MeV
Homestake Experiment	0.8
Kamiokande-II	7.5
GALLEX & GNO	0.233
SuperKamiokande	5.5
SNO	3.5
Borexino	0.15
DARWIN	0.001

GALLEX

Multiplying the average energies of ^{7}Be and pp-neutrinos (0.265 MeV and 0.812 MeV) with their respective daily event rates (0.166 events/day and 0.247 events/day) leads to a daily energy yield of 0.413 MeV. Taking the weight of the detector material (101 t) into account leads to a specific power $P' = 7.65 \times 10^{-21}$ W/t.

DARWIN

Performing the calculations on the electron-recoil spectra of the DARWIN detector leads to a possible specific power $P'_{\mathrm{pp}} = 4.01 \times 10^{-19}$ W/t for the pp-branch and $P'_{^7\mathrm{Be}} = 3.43 \times 10^{-19}$ W/t for the ^{7}Be-branch. Summing up the values from both branches, a specific power $P' = 7.44 \times 10^{-19}$ W/t is obtained. The calculated values are displayed in Table 5.5.

Table 5.5: The specific power P' for DARWIN is given in W/t for the pp and ^{7}Be-neutrino branches.

Neutrino branch	specific power P' (W/t)
pp	4.01×10^{-19}
^{7}Be	3.43×10^{-19}
Sum	7.44×10^{-19}

The specific powers of GALLEX with 7.65×10^{-21} W/t and of DARWIN, with 7.44×10^{-19} W/t are too low to power an electric vehicle.

5.2.2 Results from analysis of the neutrino energy converter

The patent assigns specific properties to the graphene that are responsible for its interaction with neutrinos. According to the standard model, electron neutrinos interact with ^{12}C and ^{13}C in the reactions in Eq. 5.1 to 5.4 [3] [28], which are listed with their corresponding neutrino threshold energy E_{th}. The threshold energies are derived from the neutrino cross sections. ^{12}C is one of three naturally occurring isotopes of carbon: while ^{12}C and ^{13}C are stable ^{14}C is radioactive with a half-life time of 5730 years.

$$^{12}C + \nu_e \longrightarrow {}^{12}N + e^- \qquad E_{th} = 17.34\,MeV \tag{5.1}$$

$$^{12}C + \nu_x \longrightarrow {}^{12}C^* + \nu_x \qquad E_{th} = 15.11\,MeV \tag{5.2}$$

$$^{13}C + \nu_e \longrightarrow {}^{13}N + e^- \qquad E_{th} = 2.22\,MeV \tag{5.3}$$

$$^{13}C + \nu_x \longrightarrow {}^{13}C^* + \nu_x \qquad E_{th} = 3.68\,MeV \tag{5.4}$$

Reaction 5.3 has the lowest threshold energy for neutrinos. This energy lies outside the range of most solar neutrino branches and only allows interactions with ^{8}B and hep-neutrinos (see Figure 5.1) [22].

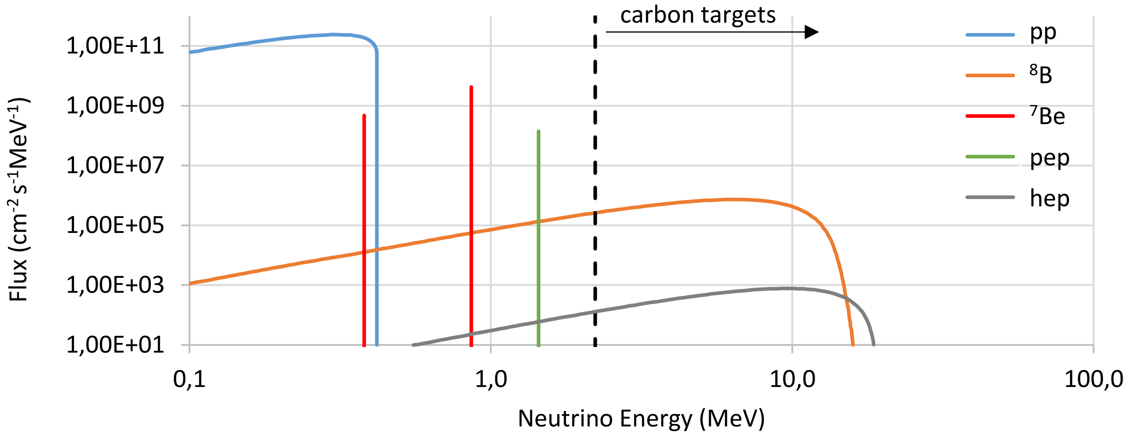

Figure 5.1: Solar neutrino energy spectrum with lowest threshold for neutrino-carbon interaction. The black dashed line visualizes the threshold energy of carbon ^{13}C targets for neutrino absorptions via reaction 5.3.

As calculated in section 4.2, energy fluxes of 8.10×10^{-2} and $1.15 \times 10^{-4}\,W/m^2$ can be expected from hep and ^{8}B-neutrinos, summing up to $0.081\,W/m^2$. This energy flux is too low to be considered for electricity generation.

The interaction of neutrinos with doped graphene is not expected to yield a significantly higher interaction rate. In doped graphene, neutrinos will interact with the dopant atoms, in addition to their interaction with carbon. The neutrino harvesting capability of the resulting graphene structure then depends on the neutrino interaction rates of both carbon atoms and dopant atoms. The results of the detector analysis in section 5.2.1 has shown that neutrino interaction rates with matter are small. Thus, neutrino interaction rates for any possible dopant will be too low to make a significant change on the neutrino harvesting abilities of the device.

6 Discussion and conclusions

The analysis of the solar neutrino energy flux on Earth and the analysis of the state-of-the-art have shown that harvesting solar neutrinos for electricity generation is no promising concept to enable sustainable transportation. This results partly from the small interaction rates of neutrinos with matter and partly from the low amount of energy released by the Sun in the form of neutrinos.

The analysis of the solar neutrino spectrum allows the estimation of the energy inherent to the solar neutrino flux on Earth. However, it does not consider the interaction probability of neutrinos with matter, which is extremely low. Still it can be used as a method to show that the solar neutrino energy flux, even in the improbable case of being fully exploited, is too low to power an electric vehicle.

During the analysis of the solar neutrino spectrum, the tool WebPlotDigitizer has proven to be valuable. It allows extracting data from figures and their usage in further calculations. In section 5.1, all deviations between reference values and calculated values based on the obtained data lie under 7%. This is relatively small compared to the discrepancy of several orders of magnitude between the power need of a car and the power potentially available from solar neutrinos. Hence, the tool's accuracy is sufficient for the purpose of this study.

Analyzing the neutrino detectors has shown that large amounts of target material are needed to capture small signals. The detectors listed in Table 5.3 range from 50 to 50 000 tonnes, a multiple of the weight of a car. As neutrinos have tiny cross sections and therefore rarely interact with matter, the energy converting efficiency of the detectors is extremely low. The fact that solar neutrino detectors, such as Borexino, need to be placed deep underground and enclosed by a water tank to shield them from natural radioactivity and cosmic rays, emphasizes on how little energy is released from neutrino interactions. Data found in literature, such as the differential electron recoil spectra in liquid xenon (shown in Fig. 4.2), allowed an approximation of the expected power output of the DARWIN detector. The results lie several orders of magnitude below a power needed to power electric vehicles.

The analysis of the neutrino energy converter has shown that neutrino-carbon interactions are not promising for converting solar neutrino energy into electricity, as their threshold energies are too high. Only the relatively low energy fluxes constituted by ^{8}B and hep-neutrinos could be (partially) exploited, depending on their interaction rates. The energy thresholds of the neutrino-carbon interactions do not give insight into the amount of energy harvested from the solar neutrino flux. To calculate this amount, the cross section for the interactions need to be determined and the interaction rate, based on the the cross section and the neutrino fluxes, calculated. For the fact that neutrino cross sections are low, regardless of the interaction, the interaction rate is expected to be too low to be worth for examination in the scope of this thesis.

For the given reasons future research in the area of solar neutrino energy harvesting for electricity generation is not recommended.

7 Outlook

As solar neutrino energy conversion technologies have not shown to be promising candidates for electricity generation, other technologies need to be explored in future studies.

Prevailing systems in sustainable transportation are based on batteries and fuel cells. However, vehicles equipped with these technologies generally range at higher prices than comparable vehicles with internal combustion engines. To further accelerate these technologies, novelties, leading to major cost reductions, are needed.

Scouting patents for emerging energy technologies in the automotive sector allows identifying innovations before they reach the market. Hence, patents published by battery and fuel cell manufactures need to be monitored closely.

Next to existing players, sustainable technology ecosystems need to be scrutinized. These ecosystems bundle experts from universities, representatives from the industry and young companies, and allow ideas to spread. University spin-offs can be promising candidates, bringing research-backed technologies to the market with the speed of a start-up. Recently published patents of such individuals, groups or companies can hint towards major breakthroughs.

Because of the nature of innovations, it is hardly possible to predict the next industry-changing novelty. Further studies evaluating patents of established and emerging players can reveal promising technologies.

Bibliography

[1] Aalbers, J. et al. “DARWIN: towards the ultimate dark matter detector”. In: *Journal of Cosmology and Astroparticle Physics* 2016.11 (2016), p. 017.

[2] Alimonti, G. et al. “The Borexino detector at the Laboratori Nazionali del Gran Sasso”. In: *Nuclear Instruments and Methods in Physics Research Section A: Accelerators, Spectrometers, Detectors and Associated Equipment* 600.3 (2009), pp. 568–593.

[3] Armbruster, B. et al. “Neutrino interactions with carbon”. In: *Nuclear Physics B - Proceedings Supplements* 38.1-3 (1995), pp. 198–203.

[4] Astroparticle Physics European Consortium. *European Astroparticle Physics Strategy 2017-2016*. 2017.

[5] Bahcall, John N. *Neutrino astrophysics*. Cambridge: Cambridge Univ. Pr, 1989.

[6] Bahcall, John N. and Serenelli, Aldo M. *How Do Uncertainties in the Surface Chemical Composition of the Sun Affect the Predicted Solar Neutrino Fluxes?* 2005.

[7] Basdevant, Jean-Louis et al. *Fundamentals In Nuclear Physics: From Nuclear Structure to Cosmology*. New York: Springer-Verlag, 2005.

[8] Bellerive, A. et al. “The Sudbury Neutrino Observatory”. In: *Nuclear Physics B* 908 (2016), pp. 30–51.

[9] Bellini, G. et al. “Final results of Borexino Phase-I on low-energy solar neutrino spectroscopy”. In: *Physical Review D* 89.11 (2014), p. 913.

[10] Berliner Korrespondentenbüro. *Neutrino Energy, der wahre Da-Vinci-Code*. Ed. by pv magazine. 2018. URL: https://www.pv-magazine.de/unternehmensmeldungen/neutrino-energy-der-wahre-da-vinci-code/.

[11] Bilenky, Samoil. *Introduction to the Physics of Massive and Mixed Neutrinos*. Vol. 947. Cham: Springer International Publishing, 2018.

[12] Boyd, Steve. *Neutrino Detectors and Sources*. 2014. URL: https://warwick.ac.uk/fac/sci/physics/staff/academic/boyd/warwick_week/neutrino_physics/lec_neutrinodetectors_writeup.pdf.

[13] Daimler AG. *The Daimler Group*. 2019. URL: https://www.daimler.com/company/.

[14] Dato, Albert et al. "Clean and highly ordered graphene synthesized in the gas phase". In: *Chemical communications (Cambridge, England)* 40 (2009), pp. 6095–6097.

[15] Demtröder, Wolfgang. *Experimentalphysik 4: Kern-, Teilchen- und Astrophysik*. Berlin, Heidelberg: Springer Berlin Heidelberg, 2017.

[16] Electric Vehicle Database. *Mercedes EQC 400 4MATIC*. 2019. URL: https://ev-database.uk/car/1135/Mercedes-EQC-400-4MATIC.

[17] European Commission. *Reducing CO2 emissions from passenger cars*. 2019. URL: https://ec.europa.eu/clima/policies/transport/vehicles/cars_en (visited on 08/13/2019).

[18] FOCUS Magazin. *Herr Krause sucht das Glück*. 2017. URL: https://www.focus.de/magazin/archiv/politik-und-gesellschaft-herr-krause-sucht-das-glueck_id_6731031.html.

[19] Groeneveld, Koert and Würth, Wolfgang. *The Mercedes-Benz EQC: Electric Intelligence*. 2019.

[20] Halzen, Francis and Klein, Spencer R. "Invited review article: IceCube: an instrument for neutrino astronomy". In: *The Review of scientific instruments* 81.8 (2010), p. 081101.

[21] Hoffmann, Kevin P. and Nestler, Ralf. *Günther Krause im Bann der Neutrinos*. 2018. URL: https://www.tagesspiegel.de/wirtschaft/strafbefehl-gegen-ex-minister-guenther-krause-im-bann-der-neutrinos/21120456.html.

[22] Ianni, A. et al. "How to observe 8B solar neutrinos in liquid scintillator detectors". In: *Physics Letters B* 627.1-4 (2005), pp. 38–48.

[23] International Energy Agency. *Global EV Outlook 2019*. 2019.

[24] IPCC. *IPCC Climate Report 2018*. Ed. by UN. 2018.

[25] Kirsten, T. et al. *Earlier Neutrino Physics Projects at MPIK*. 2019. URL: https://www.mpi-hd.mpg.de/lin/research_history.en.html#gallex.

[26] Laboratori Nazionali del Gran Sasso. *Borexino*. 2019.

[27] Lang, Peter. *YouTube Channel of Peter Lang*. 2019. URL: https://www.youtube.com/user/endingoil777.

[28] Loo, Kai. "Extending Physics Potential of Large Liquid Scintillator Neutrino Detectors". PhD thesis. University of Jyväskylä, 2016.

[29] Miramonti, Lino. *Solar neutrino detection*. 2009.

[30] NEUTRINO Germany GmbH. *Neutrino Energy, Clearly the Energy of the Future*. Ed. by PR Newswire. 2017. URL: https://www.prnewswire.com/news-releases/neutrino-energy-clearly-the-energy-of-the-future-300475268.html.

[31] Power Technology. *Neutrino energy: harnessing the power of cosmic radiation*. 2019. URL: https://www.power-technology.com/features/neutrino-energy-harnessing-the-power-of-cosmic-radiation/.

[32] Quaschning, Volker. *Understanding renewable energy systems*. London and Sterling VA: Earthscan, 2005.

[33] Reines, Fred and Cowan Jr., Clyde. "Reines-Cowan Experiments - Detecting the Poltergeist". In: *Los Alamos Science* 25 (1997).

[34] Rohatgi, Ankit. *WebPlotDigitizer*. 2019.

[35] Sanchez-Lucas, Patricia. *DARWIN: an excellent environment to probe neutrino physics*. 2018.

[36] Sanford Underground Research Facility. *Unlocking the mysteries of neutrinos*. 2017. URL: https://sanfordlab.org/feature/unlocking-mysteries-neutrinos (visited on 08/13/2019).

[37] Schubart, Holger Thorsten. "Folie aus Metall oder einer Metalllegierung". WO2016142056A1. 2016.

[38] Schulze, Heiko. *Neutrino Energy, der wahre Da-Vinci-Code / Der geheime Schlüssel liegt in Geometrie und Resonanz / Plädoyer für die Revolution der Energiezukunft*. 2018. URL: https://www.finanzen.net/nachricht/aktien/neutrino-energy-der-wahre-da-vinci-code-der-geheime-schluessel-liegt-in-geometrie-und-resonanz-plaedoyer-fuer-die-revolution-der-energiezukunft-5994689.

[39] Severino, Giuseppe. *The Structure and Evolution of the Sun*. Cham: Springer International Publishing, 2017.

[40] Suzuki, Y. “Solar Neutrinos”. In: *Space Science Reviews* 85.1/2 (1998), pp. 91–104.

[41] The DARWIN Collaboration. *DARWIN homepage*. 2019. URL: https://darwin.physik.uzh.ch/index.html.

[42] Tipler, Paul Allen and Llewellyn, Ralph A. *Modern physics*. 6th ed. New York: W. H. Freeman and Co, 2012.

Acknowledgments

First of all, I would like to thank my examiner at KTH Prof. Viktoria Martin and my supervisor at Daimler AG Thomas Nesch, who made this project possible. Without their support I wouldn't have had the necessary means to study neutrinos and neutrino energy converters.

A big thank you goes to Dr. Bernd Reinhold, who supported me in all questions regarding neutrino physics.

I also want to thank my colleagues at Lab1886, who made every day at the Lab more pleasant and cheered me up when I was struggling.

Last but not least my family was my most sturdy support and I am very grateful to have them.